De Gruyter Brill
Paradigm
ISSN 1335-8871

MEASUREMENT SCIENCE REVIEW

Journal homepage: https://reference-global.com/journal/MSR

A Digital Image Correlation Method Based on Deep Learning under Low-Light Conditions

Xiao-Yong Liu[1], Jia-Ming Hu1, Rong-Li Li[1*], Guo-Qing Han[1], Song Gao[1], ZhaoPeng Hao[1], Yuan-Ze Huang[2], Dongwei Gu[1], Cheng Zhang[1]

[1]*School of Mechanical and Electrical Engineering, Changchun University of Technology, Changchun 130012, China*
[2]*China Water Resources Dongbei Investigation, Design & Research Co., Ltd., Changchun 130021, China*

Abstract: Digital image correlation (DIC) is a widely used technique for deformation measurement, leveraging the analysis of grayscale information from surface speckle patterns to provide non-contact, full-field, and high-accuracy measurements. However, under low-light conditions, speckle images often suffer from insufficient brightness, low contrast, and significant noise, leading to degraded pattern quality and loss of critical texture information, which in turn severely undermines measurement accuracy. To address this limitation, this paper integrates deep learning-based low-light image enhancement with DIC, proposing an enhanced low-light DIC algorithm founded on EnlightenGAN, termed displacement measurement algorithm (EnDIC). A systematic performance comparison is conducted among four deep learning enhancement methods, including EnlightenGAN and Zero-Reference Deep Curve Estimation (Zero-DCE). Experimental results demonstrate that EnDIC outperforms the other methods in both image quality enhancement and displacement calculation accuracy. Furthermore, across simulated and real-world experiments under various low-light conditions, EnDIC exhibits higher measurement precision and superior robustness against illumination variations. The proposed approach thus offers a reliable and effective technical solution for engineering applications such as structural health monitoring in challenging lighting environments.

Keywords: digital image correlation, deep learning, low-light enhancement

1. INTRODUCTION

Digital image correlation (DIC) is extensively employed in various research and application fields, including advanced materials, aerospace, biomechanics, and medical imaging, owing to its merits of straightforward setup, operational simplicity, and high measurement accuracy [1]-[4]. The principle of DIC is to determine the deformed positions of individual pixels by calculating the cross-correlation of pixel grayscale values between images captured before and after deformation, thereby obtaining the displacement of the measured points. Consequently, the accuracy of DIC is critically dependent on the quality of the speckle images. Inadequate illumination, in particular, can lead to matching failures in DIC, preventing the acquisition of valid measurement results.

To ensure high speckle quality, image acquisition should ideally be conducted under sufficient and stable lighting. In practical engineering scenarios, however, images are often captured under unstable lighting, in the presence of obstructive shadows, or during nighttime operations, resulting in low-light conditions. Speckle images obtained under such circumstances suffer from insufficient brightness and pronounced noise interference, which cause a loss of fine details and texture information, ultimately increasing errors in displacement calculations.

To maintain DIC measurement accuracy in low-light environments, considerable research efforts have been devoted worldwide. Chen et al. [5] proposed an image correction algorithm based on a multi-scale bilateral filtering Retinex model. This method estimates the illumination component by integrating bilateral filtering with a multi-scale Retinex framework, introduces an adaptive 2D gamma function with correction coefficients for brightness adjustment, and finally employs CLAHE for enhancement. It effectively mitigates issues such as boundary blurring and local over-correction, thereby improving speckle image quality and enhancing the accuracy and stability of DIC measurements. Wang et al. [6] incorporated an adaptive weighting function into the sub-pixel iterative process, introducing illumination-sensitive weights to dynamically reduce the influence of high-brightness gradient regions, which improved measurement precision. Gu et al. [7] developed a correction method that combines Retinex theory with a point light source model. This approach does not require additional lighting but mathematically adjusts grayscale values. By applying a non-uniform illumination correction algorithm based on multi-scale Retinex, the effects of uneven lighting can be reduced or eliminated, thus decreasing measurement errors induced by local illumination

DOI: 10.2478/msr-2026-0036
*Corresponding author: lirl@ccut.edu.cn (R.L. Li)
© 2026 Institute of Measurement Science, SAS. This work is licensed under CC BY-NC-ND 4.0.

variations. While these methods have improved DIC performance under non-uniform lighting to some extent, in severely low-light conditions, speckle patterns become less distinct. For instance, during real-time monitoring at night, failures in speckle grayscale matching may still occur, leading to unsuccessful measurements. In such cases, enhancing low-light speckle images to improve measurement accuracy presents a viable alternative.

Traditional image enhancement techniques primarily aim to improve visual quality by redistributing pixel intensities, for example, through grayscale transformation to expand dynamic range or histogram equalization to enhance overall contrast. However, these methods suffer from notable limitations. First, most operate globally, often overlooking local image characteristics, which can result in a loss of detail or an amplification of background noise. Second, their parameters are typically set empirically, lacking an explicit model of the degradation process; consequently, their effectiveness is limited, and their robustness is insufficient when handling severely low-light images, failing to deliver consistently superior performance in challenging scenarios. More importantly, traditional methods often rely on iterative procedures, making them computationally intensive and less suitable for practical applications [8]-[10]. In recent years, with the rapid advancement of artificial intelligence, an increasing number of researchers have turned to deep learning for low-light image enhancement. A variety of deep learning-based low-light enhancement methods have been proposed, gradually establishing this approach as the mainstream in the field [11], [12]. Therefore, this paper integrates deep learning-based low-light enhancement algorithms with the DIC method to explore the potential of this synergy. Ultimately, we propose a low-light DIC displacement measurement algorithm based on EnlightenGAN, offering a novel solution for structural deformation monitoring and high-precision displacement measurement in low-light environments.

2. PRINCIPLES OF THE DIGITAL IMAGE CORRELATION METHOD

The origins of DIC can be traced back to the pioneering work in the 1980s by Peters et al. at the University of South Carolina and the Japanese researcher Ichirō Yamamoto [13], [14]. Through decades of development and refinement by researchers worldwide, DIC theory has matured into a robust technique widely employed for the precise measurement of diverse material deformations.

The DIC method determines deformation parameters by analyzing speckle pattern images of the object surface, captured by a CCD/CMOS camera before and after loading. The image acquired prior to loading is termed the reference image, while the image captured post-loading is the deformed image. The core computational principle is illustrated in Fig. 1. In the reference image, a square region of $(2N+1)\times(2N+1)$ pixels centered on a point of interest $P(x_i, y_i)$ is defined as the reference subset, denoted $f(x, y)$. Correspondingly, a larger square search subset of $(2M+1)\times(2M+1)$ pixels (with $M > N$) is established in the deformed image, centered on the approximate location of P. Within this search subset, every possible square region of the same size as the reference subset is considered a deformed subset, $g(x', y')$. A predefined correlation function (e.g., zero-mean normalized cross-correlation (ZNCC)) is then computed between the reference subset f and each candidate deformed subset g within the search area, generating a correlation coefficient map. In the figure, $\otimes$ is used to represent the relevant calculations. The position yielding the maximum (or minimum) correlation coefficient identifies the location of the target subset. The displacement vector d for point P is given by the coordinate difference between the center of this target subset, $P'(x_i', y_i')$, and the center of the original reference subset. By repeating this process for all pixel points (or a grid of points) across the image, the full-field displacement of the specimen surface is obtained.

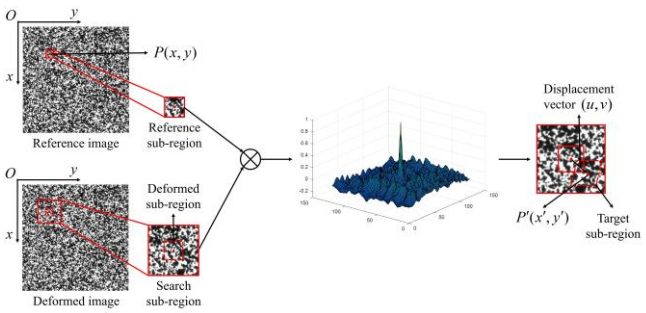

Fig. 1. Schematic diagram of the DIC method.

The Newton–Raphson (N-R) iterative algorithm is central to DIC for its second-order convergence, enabling efficient and accurate resolution of the nonlinear least-squares optimization problem inherent in sub-pixel-level displacement and strain measurements [15]. By incorporating second-order derivative information (the Hessian matrix) of the correlation function near the solution estimate, this method significantly improves both the stability and the convergence speed.

Within the N-R framework, the ZNCC function is commonly adopted as the matching criterion [16]:

$$C(X) = \frac{\sum_{i=1}^{n}\{[f(x_i,\ y_i) - f_m] \times [g(x_i', y_i') - g_m]\}}{\sqrt{\sum_{i=1}^{n}[f(x_i, y_i) - f_m]^2}\sqrt{\sum_{i=1}^{n}[g(x_i', y_i') - g_m]^2}} \quad (1)$$

In this equation, $f(x_i, y_i)$ and $g(x_i', y_i')$ represent the grayscale intensities at locations (x_i, y_i) and (x_i', y_i') within the reference and deformed subsets, respectively. The terms f_m and g_m denote the corresponding mean gray values of these subsets, n is the total number of pixels within a subset, and $\boldsymbol{X}$ is the vector of unknown deformation parameters. The displacement mapping between a point (x_i, y_i) in the reference subset and its counterpart (x_i', y_i') in the deformed subset is described by a first-order shape function:

$$\begin{cases} x_i' = x_i + u + u_x \Delta x_i + u_y \Delta y_i \\ y_j' = y_j + v + v_x \Delta x_i + v_y \Delta y_i \end{cases} \quad (2)$$

where u and v are the integer-pixel displacements of the subset center (the point to be determined) in the x and y directions; u_x, u_y, v_x, and v_y are the first-order displacement gradients; and Δx_i and Δy_i are the distances from point (x_i, y_i) to the subset center.

The N-R algorithm iteratively solves for the parameter vector $\boldsymbol{X}$ that maximizes (or minimizes) the correlation coefficient C. The iterative update formula is:

$$\boldsymbol{X}^{(k+1)} = \boldsymbol{X}^{(k)} - \frac{\nabla C\left(\boldsymbol{X}^{(k)}\right)}{\nabla\nabla C(\boldsymbol{X}^{(k)})} \tag{3}$$

Here, $\boldsymbol{X}^{(k)}$ and $\boldsymbol{X}^{(k+1)}$ are the parameter vectors at the k-th and $(k+1)$-th iterations, respectively; ∇C is the first-order derivative of the correlation coefficient (i.e., the gradient vector); and $\nabla C\nabla C$ is its second-order derivative (i.e., the Hessian matrix).

To achieve sub-pixel precision, grayscale intensities at non-integer locations within the deformed subset are required. These are obtained via bicubic spline interpolation [17]. The one-dimensional cubic spline interpolation function is expressed as:

$$\begin{aligned} S(x) = {} & [1 + 2(x - x_{h+1})] \cdot (x - x_{h+2})^2 f_{h+1} \\ & + [1 - 2(x - x_{h+2})] \cdot (x - x_{h+1})^2 f_{h+2} \\ & + (x - x_{h+1}) \cdot (x - x_{h+2})^2 \cdot S'(x_{h+1}) \\ & + (x - x_{h+2}) \cdot (x - x_{h+1})^2 \cdot S'(x_{h+2}) \end{aligned} \tag{4}$$

where x_{h+1} and x_{h+2} are two adjacent known pixel coordinates, f_{h+1} and f_{h+2} are the corresponding grayscale values, $S(x)$ is the interpolating function, $S'(x_{h+1})$ and $S'(x_{h+2})$ are its derivatives at the endpoints. Extending this formulation to two dimensions yields the bicubic spline interpolation expression:

$$S(x, y) = \sum_{h=0}^{3} \sum_{l=0}^{3} a_{hl}\, x^h y^l \tag{5}$$

where a_{mn} are the coefficients containing derivative information. Determining these coefficients requires applying boundary conditions. Using the first-type (gradient) boundary condition:

$$\begin{cases} S^{'} = g_0{}^{'} \\ S_3{}^{'} = g_3{}^{'} \end{cases} \tag{6}$$

where f_x' and f_y' denote the grayscale gradients at the boundary pixels. Equation (6) indicates that the bicubic spline interpolation process requires the computation of image gradients at the boundaries.

3. PRINCIPLES OF FOUR COMMON DEEP LEARNING LOW-LIGHT ENHANCEMENT METHODS

Ensuring the accuracy and robustness of DIC in low-light environments hinges critically on the effective enhancement of the acquired speckle images. In recent years, deep learning-based methods for low-light image enhancement have emerged as a prominent research focus, owing to their formidable capacity for feature learning and nonlinear mapping. Typically, independent of explicit physical illumination models or paired training data, these methods can adaptively restore image brightness, contrast, and detail, demonstrating strong generalization in complex real-world scenarios. Given this capability, this section focuses on four representative deep learning-based enhancement methods deemed suitable for DIC applications: EnlightenGAN [18], Zero-Reference Deep Curve Estimation (Zero-DCE) [19], Self-Calibrated Illumination (SCI) [20], and Illumination-aware and Context-aware Enhancement Network (IceNet) [21], [22]. These approaches, which are based on distinct technical paradigms such as generative adversarial networks (GAN), curve estimation, illumination decomposition, and interactive enhancement, each possess unique characteristics. Their fundamental principles, network architectures, and loss function designs are systematically elaborated below, laying the groundwork for the subsequent experimental analysis of their integration with DIC. The code for the comparison method can be obtained from the cited references.

A. EnlightenGAN

EnlightenGAN is an unsupervised low-light image enhancement method built upon GAN. Its core premise is to train a generator network, via adversarial learning, to map a low-light input image to its normally illuminated counterpart without requiring strictly paired training data. The framework comprises two main components: A U-Net-structured generator and a discriminator featuring a global-local architecture.

The generator employs an encoder-decoder design with skip connections to preserve fine image details. During training, it takes a low-light image as input and produces an enhanced output. Its key innovations lie in two aspects. First, it introduces a Self Feature Preserving Loss, which constrains content consistency by measuring the cosine similarity between the input and output images in the deep feature space of a pre-trained Visual Geometry Group (VGG) network, effectively mitigating color distortion and detail loss. Second, it adopts a dual-discriminator strategy comprising a global discriminator that assesses the overall naturalness of the illumination and a local discriminator that focuses on randomly sampled patches, compelling the generator to produce realistic textures and details locally. By jointly optimizing the adversarial loss, the self-feature-preserving loss, and the conventional perceptual loss, EnlightenGAN achieves high-quality unsupervised enhancement, demonstrating particular efficacy in handling scenes with non-uniform illumination.

B. Zero-Reference Deep Curve Estimation

Zero-DCE presents a zero-reference learning framework for low-light enhancement via deep curve estimation. Its most distinctive feature is that its training process dispenses with the need for any paired normal-light images for supervision. This approach deviates from the conventional end-to-end image-to-image mapping paradigm, instead learning a set of pixel-wise, high-order curves that dynamically adjust the input image's tonal values.

Specifically, the Zero-DCE network is a lightweight deep model that takes a low-light image and predicts, for each pixel, a set of parameters defining a pixel-wise adjustment curve. This curve is applied iteratively to adaptively expand the image's dynamic range. The training is guided solely by a set of carefully crafted non-reference loss functions. These include:

i. *A Spatial Consistency Loss* to preserve the relative illumination relationships between neighboring regions;
ii. *An Exposure Control Loss* that constrains the average intensity of local areas to a medium gray level to rectify under-/over-exposure;
iii. *A Color Constancy Loss* based on the gray-world assumption to mitigate color casts; and
iv. *An Illumination Smoothness Loss* to enforce spatial smoothness on the estimated curve parameters. Through this unique strategy of curve estimation and reference-free optimization, Zero-DCE achieves efficient enhancement with a low parameter count and good generalization.

C. Self-Calibrated Illumination

The SCI method is a deep learning enhancement framework centered on a self-calibration module, drawing inspiration from iterative optimization in image processing. Its core innovation is a lightweight, iterative network structure that progressively refines the enhancement result across multiple stages, each incorporating a SCI module.

The network consists of several identical cascaded stages, each containing an encoder for feature extraction and a decoder for image reconstruction. Embedded within each stage's feature space, the SCI module explicitly models and adjusts the illumination component. It first estimates a coarse initial illumination map from global features using operations such as average pooling. A calibration sub-network then refines this map by interacting with the original features, producing a more accurate illumination calibration map. Finally, this refined map is used to adaptively correct the features, achieving illumination equalization at the feature level. This multi-stage, coarse-to-fine self-calibration mechanism enables effective separation and correction of illumination. Trained in an unsupervised manner using a combination of smoothness, reconstruction, and adversarial losses, SCI ensures the enhanced images maintain a natural appearance and rich texture details.

D. Illumination-aware and Context-aware Enhancement Network

IceNet is a dual-branch architecture grounded in a refined Retinex theory, concurrently addressing illumination awareness and contextual information. It explicitly decomposes an image into an illumination map and a reflectance map, attributing the low-light problem primarily to degraded illumination.

The network begins by extracting multi-scale features via a shared encoder. These features are then processed by two parallel, interacting branches: An Illumination Adjustment Branch and a Reflectance Restoration Branch. The former estimates a transformation map to correct illumination, using mechanisms such as Long Short-Term Memory to model global illumination context and generate physically plausible, smooth enhancement coefficients. The latter focuses on restoring surface texture and color information from the reflectance component, often employing a densely connected structure with attention mechanisms to capture critical details. The outputs from both branches are fused in a decoder to reconstruct the final enhanced image. IceNet is optimized with a multi-task loss function, including an illumination smoothness loss for the illumination map, a texture preservation loss for the reflectance map, and perceptual and color fidelity losses for the final output. This explicit decomposition and cooperative dual-branch design enable IceNet to handle extreme low-light conditions more effectively, enhancing brightness while suppressing noise and preserving color authenticity.

4. ESTABLISHMENT OF A DEEP LEARNING-ENHANCED LOW-LIGHT DIC ALGORITHM

A. Comparative performance evaluation of four low-light enhancement algorithms

While EnlightenGAN has demonstrated superior performance in enhancing natural low-light images, its efficacy for DIC-specific speckle images requires careful examination. Speckle images, serving as the measurement carrier in DIC, possess distinct characteristics: their value lies not in visual content, but in high-contrast, random grayscale texture patterns; sub-pixel DIC accuracy critically depends on preserving subtle local grayscale gradients; and they exhibit low tolerance to artifacts (e.g., over-smoothing or texture distortion) introduced by enhancement algorithms. Thus, whether EnlightenGAN's advantage extends to the DIC context — specifically in preserving critical speckle texture, maximizing feature information content, and ultimately improving displacement measurement accuracy — remains a pivotal question.

To address this, a comprehensive comparative analysis of EnlightenGAN, Zero-DCE, SCI, and IceNet was conducted. The evaluation employed peak signal-to-noise ratio (PSNR) and structural similarity index (SSIM) to measure the fidelity and structural similarity between enhanced images and ground-truth normal-light reference images (available in controlled simulations). Higher values for these metrics indicate results closer to the ideal reference. Furthermore, considering the unique requirements of DIC, two additional feature-oriented metrics were introduced: The mean intensity gradient (MIG) and Shannon entropy. MIG reflects the overall intensity gradient strength of an image, where a higher value suggests richer local features, which are crucial for reliable subset matching in DIC. Shannon entropy quantifies the randomness and information content of the gray-level distribution; a higher entropy value typically correlates with greater feature uniqueness and is associated with potentially higher DIC calculation accuracy and reliability.

The PSNR, which indicates better image quality when higher, is calculated from the mean squared error (MSE), as shown in (7) and (8), respectively. SSIM, ranging from 0 to 1 with higher values denoting better quality, is computed using (9). For DIC-specific assessment, MIG — proposed by Pan et al. [23] to evaluate overall speckle pattern quality — is

defined by (10). A larger MIG signifies better suitability for DIC. Liu et al. [24] used Shannon entropy (H), defined in (11), to assess speckle pattern quality, concluding that higher entropy yields greater measurement accuracy, as it indicates a more random pixel intensity distribution and greater information content within the speckle subset.

$$PSNR = 10\,log_{10}\left(\frac{{I_{max}}^2}{MSE}\right) \tag{7}$$

where ${I_{max}}^2$ is the square of the maximum pixel value in the image. The formula for MSE is as follows:

$$MSE = \frac{\sum_{i=1}^{M}\sum_{j=1}^{N}\,[f(i,j) - g(i,j)]^2}{M \cdot N} \tag{8}$$

where, $f(i,j)$ and $g(i,j)$ are the gray values at point (i,j) in the original image and the evaluated image, respectively.

$$SSIM = \left(\frac{2\mu_x\mu_y + C_1}{{\mu_x}^2 + {\mu_y}^2 + C_2}\right)\left(\frac{2\sigma_{xy} + C_2}{{\sigma_x}^2 + {\sigma_y}^2 + C_2}\right) \tag{9}$$

where, μ_x and μ_y are the means of the images; σ_x and σ_y are the variances of the images; σ_{xy} is the covariance of the images; C_1 and C_2 are constants to prevent the denominator from being zero.

$$\delta_f = \frac{\sum_{i=1}^{W}\sum_{i=1}^{H}\left|\nabla f(x_{ij})\right|}{W \times H} \tag{10}$$

where W and H represent the width and height of the speckle image, $\left|\nabla f(x_{ij})\right| = \sqrt{f_x(x_{ij})^2 + f_y(x_{ij})^2}\,|\nabla f|$ is the magnitude of the gray gradient vector at each pixel point, with $f_x(x_{ij})$ and $f_y(x_{ij})$ being the gray derivatives of pixel point x_{ij} in the x and y directions.

$$S = -\sum_{j=0}^{2^{\beta}-1} P(a_j)\,log[P(a_j)] \tag{11}$$

where S is the Shannon entropy of the image; β is the bit depth of the image (typically, actually acquired images are 8-bit, so $\beta = 8$). According to the definition of image entropy, a larger entropy of the speckle subset indicates more pronounced randomness in the gray distribution of its pixels and greater information content.

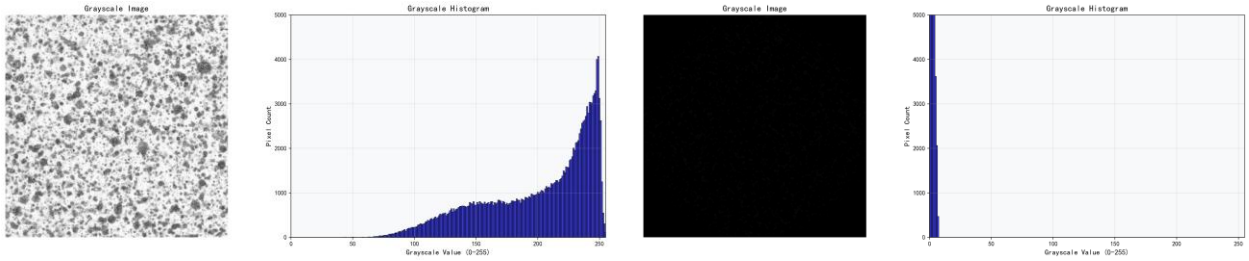

(a) (b)

Fig. 2. Simulated reference speckle pattern (a), low-illumination speckle pattern (b), and their gray histograms.

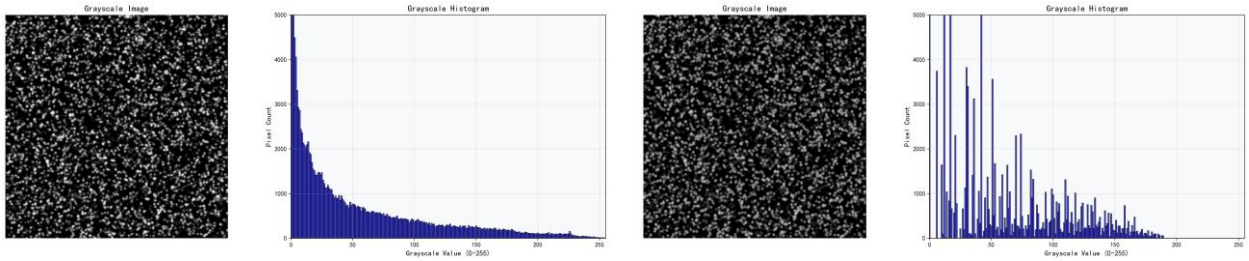

(a) EnlightenGAN (b) Zero-DCE

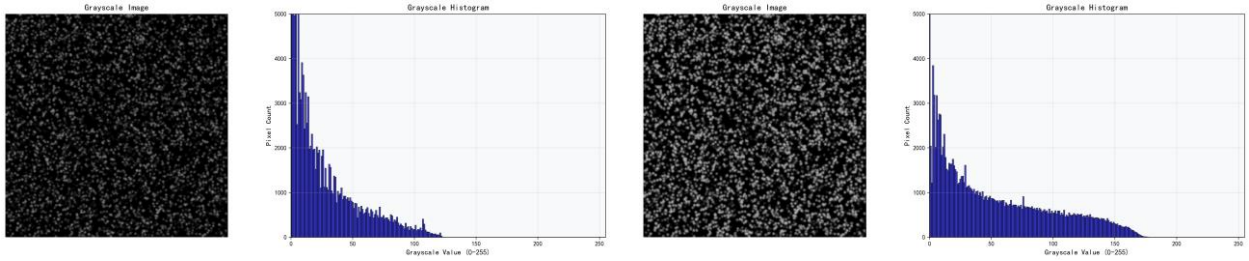

(c) SCI (d) IceNet

Fig. 3. Comparison of simulated speckle enhancement results and gray histograms.

The evaluation first utilized simulated speckle images. Patterns were generated using the method proposed by Zhou et al. [25] and subsequently degraded with simulated illumination to create low-light conditions. Fig. 2 presents the original reference speckle pattern, the corresponding low-light pattern, and their respective grayscale histograms. To compare the enhancement effects, the low-light speckle images were processed through the pre-trained models of the four algorithms. The visual enhancement results for the simulated case are compared in Fig. 3, and the corresponding quantitative metrics (MIG, Shannon entropy, PSNR, SSIM) are summarized in Table 1.

To assess performance under practical conditions, real speckle images were captured without providing stable artificial lighting, simulating a nighttime or low-light engineering environment. Fig. 4 shows the real reference and low-light speckle patterns along with their histograms. The enhancement results on these real images are presented in Fig. 5, with the quantitative evaluation detailed in Table 2.

Table 1. Comparison of simulation speckle evaluation indicators.

Algorithm	MIG	Shannon entropy	PSNR	SSIM
EnlightenGAN	22.54	6.34	28.02	0.87
Zero-DCE	20.58	5.88	22.35	0.83
SCI	17.52	5.46	21.25	0.81
IcNET	16.14	5.47	20.11	0.77

Table 2. Comparison of real speckle evaluation indicators.

Algorithm	MIG	Shannon entropy	PSNR	SSIM
EnlightenGAN	17.33	6.52	22.31	0.84
Zero-DCE	12.22	5.84	20.03	0.79
SCI	10.28	5.88	18.12	0.74
IcNET	9.34	5.82	12.83	0.75

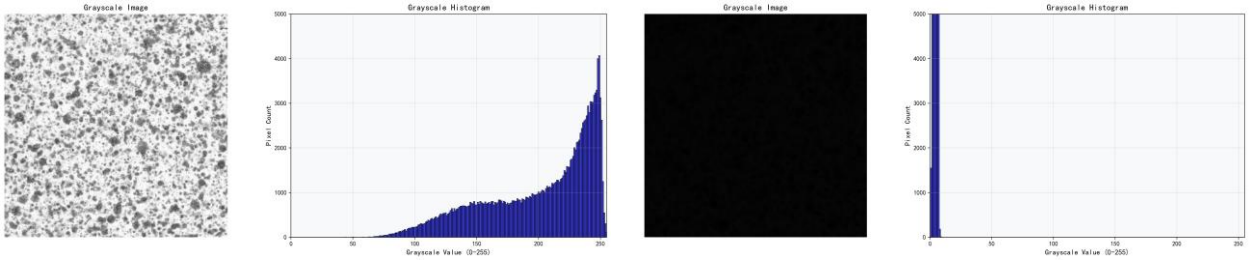

(a) (b)

Fig. 4. The true reference speckle pattern, the low-illumination speckle pattern, and their grayscale histograms.

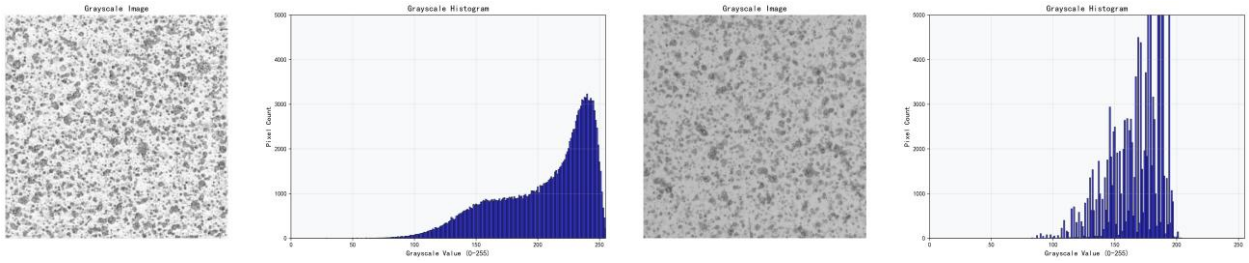

(a) EnlightenGAN (b) Zero-DCE

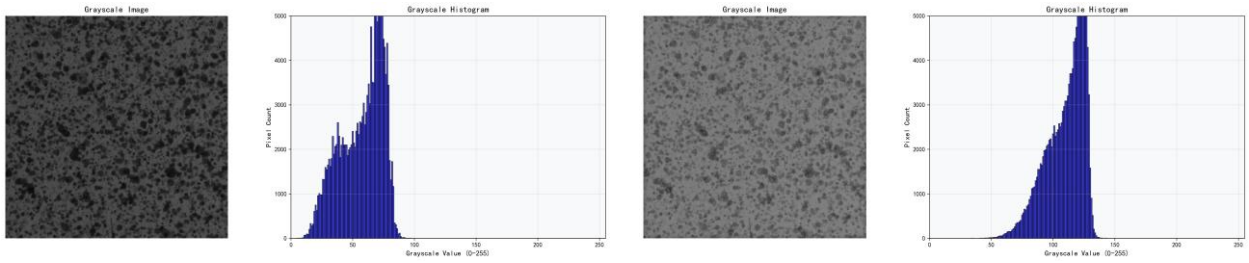

(c) SCI (d) IceNet

Fig. 5. Comparison of the actual speckle enhancement results.

A comparative analysis of the result images clearly shows that, for both simulated and real speckle patterns, the images restored by the EnlightenGAN algorithm exhibit superior visual quality, with more effectively recovered detail and texture information. This visual assessment is strongly corroborated by the quantitative data. As shown in Table 1 and Table 2, EnlightenGAN consistently achieves the highest SSIM and PSNR scores, indicating that its outputs are most structurally similar to the reference images and exhibit the smallest error. Furthermore, EnlightenGAN-processed

images also yield the highest MIG and Shannon entropy values, confirming they possess the richest local gradient features and the greatest information content. These results collectively demonstrate that the EnlightenGAN algorithm provides the highest enhancement quality for low-light speckle images among the methods compared, making it the most suitable candidate for integration with DIC.

B. Digital image correlation method based on EnlightenGAN low-light enhancement

When traditional low-light enhancement algorithms are integrated with DIC, they typically use a serial processing approach: "enhance first, then calculate." In this mode, the image enhancement module and the displacement solving module are independent of each other, each with different optimization objectives: enhancement algorithms often aim to improve visual quality or general image metrics, whereas the DIC algorithm pursues the accuracy of the displacement field calculation. The separation of the two modules may lead to a situation where the enhanced image shows improved visual quality but fails to optimally serve the subsequent key requirement of displacement solving, posing a potential problem of inconsistent optimization objectives.

To achieve synergistic optimization of image quality improvement and displacement calculation accuracy enhancement, this paper proposes a DIC method based on EnlightenGAN low-light enhancement (EnDIC). When applying the deep learning low-light enhancement model to the DIC workflow, the training parameters are continuously adjusted around the practical task-oriented objective of "displacement error" to obtain optimal performance in the DIC field. The overarching process for establishing the EnDIC algorithm is illustrated in Fig. 6.

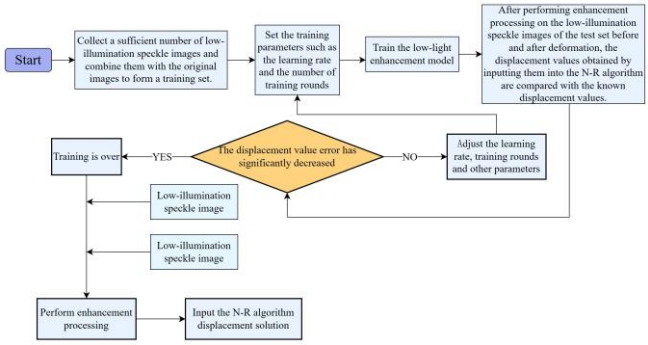

Fig. 6. The flowchart of the EnDIC algorithm.

To rigorously and comprehensively evaluate the actual improvement in DIC calculation accuracy afforded by the enhancement algorithms, this study uses a dual validation strategy comprising simulated and real experiments. Simulated experiments provide an idealized benchmark with precisely known displacement fields, allowing for quantitative analysis of absolute accuracy gains. Real experiments are then used to verify the algorithm's effectiveness and robustness in complex, practical application scenarios.

5. EXPERIMENTAL VERIFICATION

A. Simulated experiment analysis

To isolate the impact of image quality on measurement accuracy from confounding factors such as loading inhomogeneity and system vibrations present in real tests, controlled simulated translation and rotation experiments were conducted. Following the method by Zhou et al., a simulated speckle pattern was generated and treated as the undeformed reference image. Nine deformed images were created by digitally translating this reference image from 0.1 to 0.9 pixels along the x-axis via interpolation. All ten images were then subjected to simulated illumination degradation to create low-light conditions. These images were processed using the four enhancement algorithms, and DIC calculations were performed on the enhanced outputs. The resulting absolute mean errors and standard deviations for the translation measurements are presented in Fig. 7.

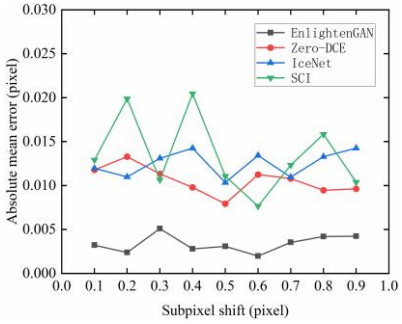

(a) Absolute mean error

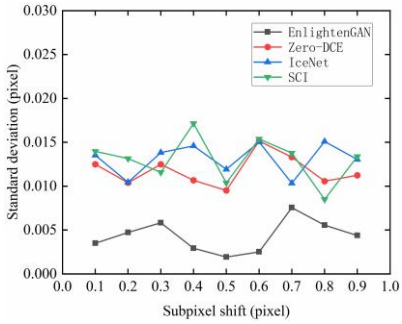

(b) Standard deviation

Fig 7. The results of the simulation translation experiment.

For the rotation experiment, the reference image was rotated counterclockwise about its center by angles incrementally increasing from 0.1° to 0.9°, generating nine deformed images. After applying the same low-light simulation, the set of ten images was enhanced by the four algorithms and analyzed via DIC. The absolute mean errors and standard deviations for the rotation angle measurements are shown in Fig. 8.

As evidenced by Fig. 7 and Fig. 8, the EnlightenGAN-enhanced speckle images yield significantly lower absolute mean errors and standard deviations for both sub-pixel translation and rotation measurements than those processed by Zero-DCE, SCI, and IceNet. Notably, within the 0.1 to 0.9-pixel translation range, the error curve of the EnDIC algorithm exhibits reduced fluctuations and higher

stability, indicating its superior ability to restore critical texture and gradient information under low-light conditions. The enhanced consistency in angle measurement further underscores EnlightenGAN's effectiveness. These results confirm that in an ideal, controlled setting, EnlightenGAN not only improves visual quality but also substantially enhances the measurement accuracy and reliability of the DIC system, providing a solid foundation for its application in real-world low-light scenarios.

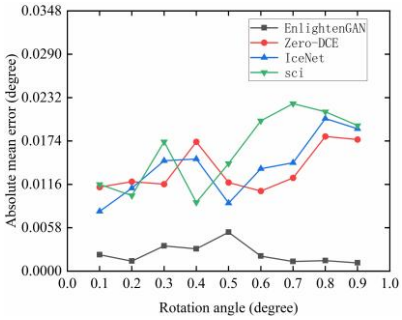

(a) Absolute mean error

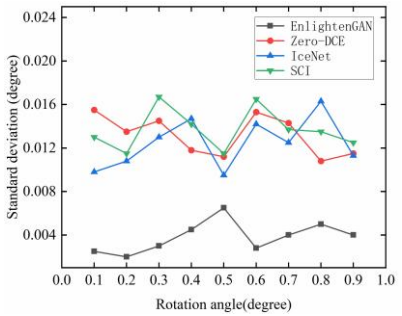

(b) Standard deviation

Fig. 8. The results of the simulated rotation experiment.

B. Real experiment analysis

To evaluate the robustness of the algorithms against practical environmental disturbances (e.g., illumination variation, noise) and compare their measurement accuracy under real conditions, rigid-body translation and rotation experiments were performed on a physical specimen. The acquisition system, depicted in Fig. 9, consisted of a translation/rotation stage, an MV-CS050-10UC CCD camera, an LED light source, the speckle-coated specimen, and a control computer.

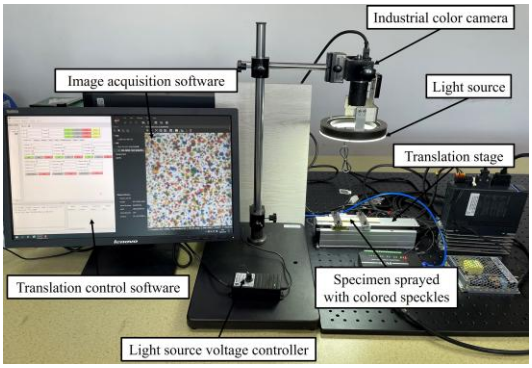

Fig. 9. Speckle image acquisition system.

For the translation test, the specimen was displaced from 0.1 mm to 0.9 mm via the computer-controlled stage. The light source was deactivated during acquisition to simulate a nighttime low-light monitoring scenario. The captured speckle images were processed using the four enhancement algorithms prior to DIC displacement calculation. The absolute mean errors and standard deviations are plotted in Fig. 10.

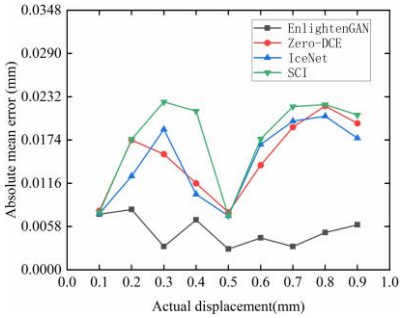

(a) Absolute mean error

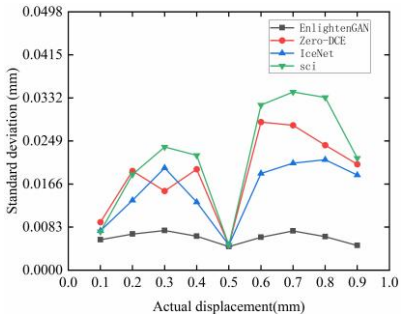

(b) Standard deviation

Fig. 10. The results of the real translation experiment.

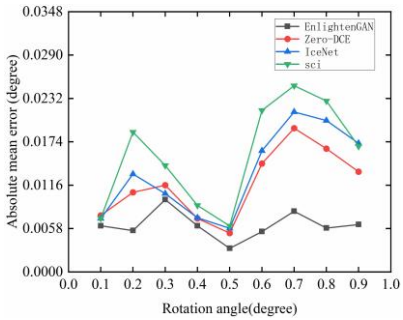

(a) Absolute mean error

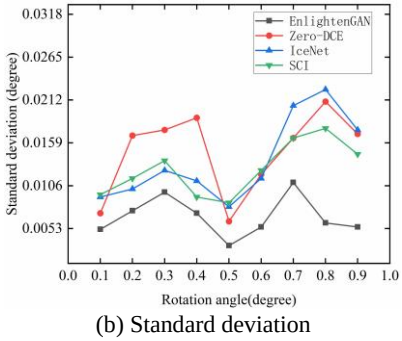

(b) Standard deviation

Fig. 11. The results of the actual rotation experiment.

Similarly, for the rotation test, the specimen was rotated from 0.1° to 0.9°. With the light source switched off, the captured low-light images were enhanced and then analyzed. The absolute mean errors and standard deviations for the rotation measurements are shown in Fig. 11.

The results in Fig. 10 and Fig. 11 demonstrate that, even without stable illumination, EnlightenGAN-preprocessed images maintain high measurement accuracy in DIC. Both the absolute mean error and standard deviation are significantly lower than those from the other three algorithms. Furthermore, the EnDIC error curve shows minimal fluctuation with increasing displacement, indicating excellent system stability. Consistent performance in the rotation experiment confirms its robustness for angular measurements. These findings validate the effectiveness of EnlightenGAN in enhancing real low-light speckle images and underscore the strong anti-interference capability and practical reliability of the proposed EnDIC algorithm, positioning it as a viable high-precision solution for deformation monitoring in challenging low-light environments such as nighttime or darkroom settings.

C. Algorithm stability analysis

While previous experiments established EnlightenGAN's superiority under uniformly low-light conditions, its robustness under varying illumination required further investigation. An additional experiment was designed to test stability under controlled changes in illumination.

A voltage-controlled LED source provided adjustable brightness. Initially, the accuracy of the EnDIC algorithm was directly compared against the standard N-R algorithm applied to raw images captured at a fixed 11 V setting (for translations from 0.1 to 0.9 pixels). The comparison (Fig. 12) shows that the EnDIC-based method delivers more credible and stable results in both simulated and real experiments.

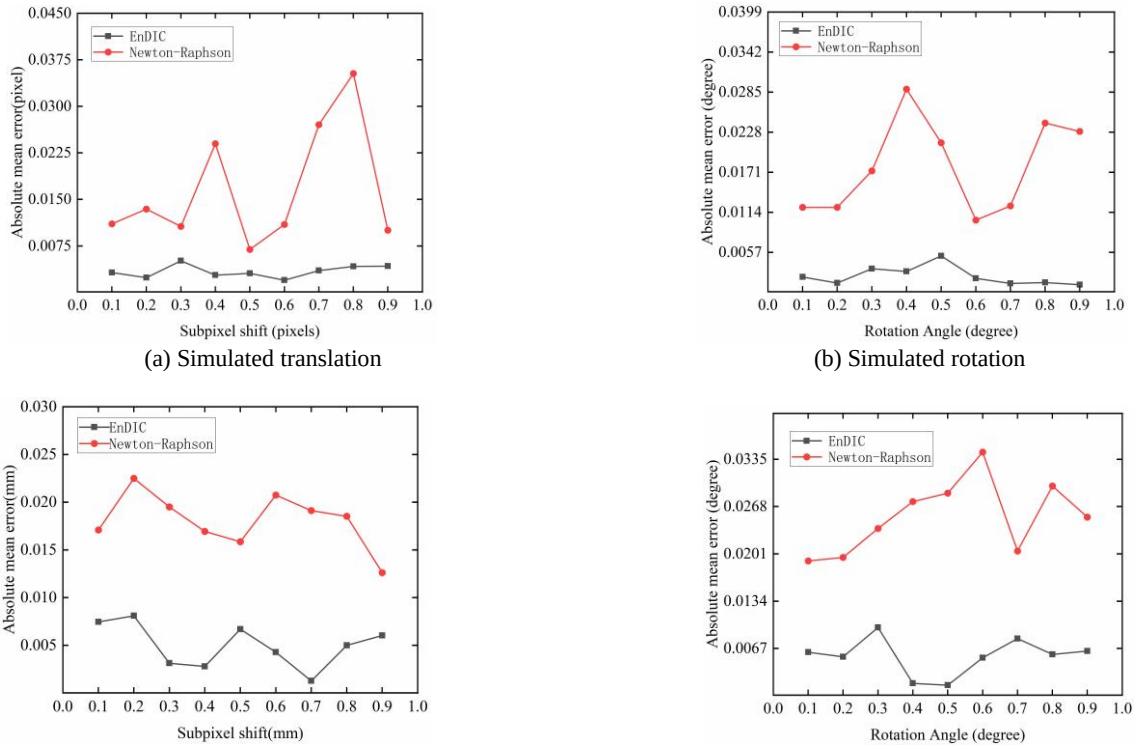

(a) Simulated translation

(b) Simulated rotation

(c) True translation

(d) True rotation

Fig. 12. The absolute mean error results of the calculation for low-illumination speckle images.

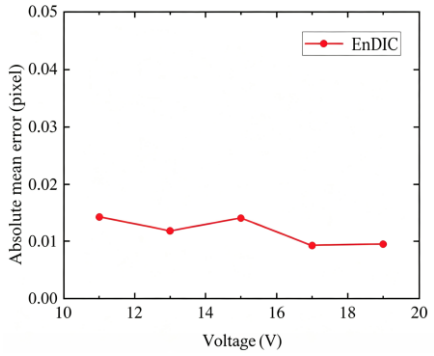

Fig. 13. The absolute mean error calculated by the algorithm for a translational displacement of 0.9 pixels under different voltages.

To explicitly test illumination robustness, speckle images were captured under different source voltages (simulating different illumination levels). The mean error for a 0.9-pixel translation, measured by EnDIC across these conditions, is plotted in Fig. 13. Corresponding sample speckle patterns and their enhanced versions are listed in Table 3. The relatively weak fluctuations in measurement error across illumination levels (Fig. 13) provide direct evidence of the EnDIC algorithm's robustness to illumination changes.

In summary, conclusions from both ground-truth-based simulations and practical real experiments are consistent: For DIC analysis of low-light speckle images, the EnDIC algorithm — which incorporates EnlightenGAN preprocessing — achieves significantly superior computational

accuracy, reliability, and noise resistance compared to traditional DIC applied directly to low-light images. It also demonstrates reduced sensitivity to illumination variations. The fundamental reason lies in EnlightenGAN's data-driven ability to recover the high-frequency texture and gradient information crucial for DIC's sub-pixel matching, which is often lost in dim environments, while simultaneously suppressing noise. By providing higher-quality, feature-sharpened input to the DIC solver, the integrated approach fundamentally improves measurement fidelity. Therefore, integrating EnlightenGAN as a preprocessor is a highly promising strategy for reliably extending the application boundaries of DIC technology to demanding low-light industrial and field settings.

Table 3. Speckle patterns under different lighting conditions and their processing results.

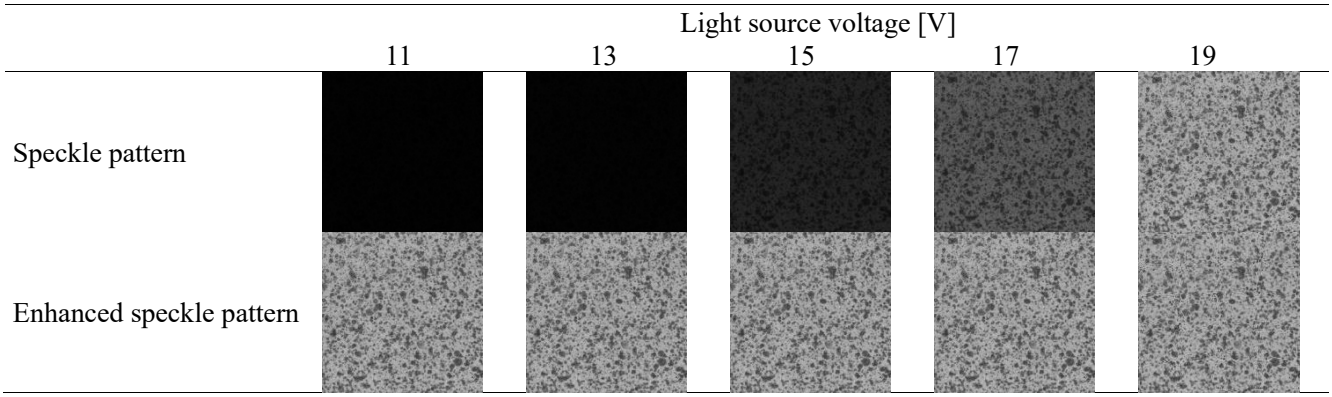

6. Conclusion

Images captured under low-light conditions frequently suffer from inadequate brightness and loss of critical features, severely compromising measurement accuracy. To address this challenge, this paper integrates deep learning-based low-light image enhancement with DIC, proposing a novel low-light DIC EnDIC based on EnlightenGAN. Comprehensive experiments involving both image quality assessment and displacement calculation accuracy lead to the following conclusions:

Compared to the other three low-light enhancement algorithms (Zero-DCE, SCI, and IceNet), speckle images processed by EnlightenGAN achieve the highest PSNR, an SSIM value closest to 1 (indicating superior structural similarity to the reference), and the highest MIG and Shannon entropy. This demonstrates that EnlightenGAN best preserves speckle texture, enhances local gradients, and maximizes feature information content — all of which are critical for DIC. Consequently, in sub-pixel displacement calculations, EnDIC reduced the absolute mean error by 30 % in simulated experiments and decreased the standard deviation of the displacement field by 24.3 % in real experiments. Across both simulated and real translation/rotation tests, EnlightenGAN-enhanced images consistently yielded higher accuracy and lower error in DIC analysis, validating its practical efficacy.

The proposed EnDIC algorithm significantly enhances the robustness and accuracy of DIC measurements in low-light environments, maintaining stable performance even under varying illumination. In summary, EnlightenGAN exhibits distinct advantages over comparable methods in terms of detail preservation, illumination uniformity, and measurement stability. This work successfully addresses the problem of speckle detail loss in low-light conditions, providing a reliable technical solution for structural health monitoring and material deformation analysis in challenging lighting scenarios, with considerable engineering application value.

Acknowledgment

This work was supported in part by the Natural Science Foundation of Jilin Province, China (Grant No. 20230101215JC); Science and Technology Research Project of Jilin Provincial Department of Education, China (Grant No. JJKH20230757CY).

References

[1] Gong, W., Ding, K., Wang, X., Shao, X., Gao, F. (2023). Research status and prospect of high-temperature digital image correlation methods for aircraft. *Intensity and Environment*, 50 (5), 43-53. (in Chinese) https://doi.org/10.19447/j.cnki.11-1773/v.2023.05.006

[2] Liu, X. (2012). *Digital image correlation method and its application in mechanical property testing of materials*. Thesis, Jilin University, Changchun, China. (in Chinese)

[3] Yang, J., Chen, H., Zhang, F. (2023). Research on vehicle tracking system in complex scenarios. *Electronic Products World*, 30 (7), 33-36. (in Chinese)

[4] Su, Z., Wang, W., Sun, J. et al. (2024). Application research on deformation measurement methods in geomechanical model experiments. *Geological Review*, 70 (1), 287-308. (in Chinese) https://doi.org/10.16509/j.georeview.2023.09.001

[5] Chen, S., Wen, Y., An, H. (2025). Correction of non-uniform illumination speckle images based on multi-scale bilateral filtering Retinex. *Laser Technology*, 49 (1), 33-40. (in Chinese)

[6] Wang, L., Wan, Q., Wei, L. et al. (2019). Influence of correlation function with weighting factor on the performance of digital image algorithm. *Journal of Chengdu University (Natural Science Edition)*, 38 (4), 346-350. (in Chinese)

[7] Gu, G., She, B., Xu, G., Xu, X. (2017). Non-uniform illumination correction based on the retinex theory in digital image correlation measurement method. *Optica Applicata*, 47 (2), 199-208. https://doi.org/10.5277/oa170203

[8] Geng, X. (2022). Review of low-light image enhancement algorithms. *Shanxi Electronic Technology*, 6, 86-89. (in Chinese)

[9] Lyu, Z., Niu, H., Sun, F., Zhen, T. (2025). Review of research on low-light image enhancement algorithms. *Infrared Technology*, 47 (2), 165-178. (in Chinese)

[10] Tang, H., Zhu, H., Xie, C. (2022). Low illumination image enhancement method review. *Journal of Forestry Machinery and Woodworking Equipment*, 50 (7), 4-10. (in Chinese) https://doi.org/10.13279/j.cnki.fmwe.2022.0114

[11] Chen, Z., Yang, J., Li, F., Feng, Z. (2025). Review on deep learning-based key algorithm for train running environment perception. *Journal of Zhejiang University (Engineering Science)*, 59 (1), 1-17. (in Chinese) https://doi.org/10.3785/j.issn.1008-973X.2025.01.001

[12] Li, Z., Liu, J., Yang, H., Zhang, Z. (2024). Review of low-illuminance image enhancement algorithm based on deep learning. *Journal of Applied Optics*, 45 (6), 1095-1107. (in Chinese) https://dx.doi.org/10.5768/JAO202445.0609001

[13] Peters, W. H., Ranson, W. F. (1982). Digital imaging techniques in experimental stress analysis. *Optical Engineering*, 21 (3), 427-431. https://doi.org/10.1117/12.7972925

[14] Yamaguchi I. (1981). A laser-speckle strain gauge. *Journal of Physics E: Scientific Instruments*, 14 (11), 1270. https://doi.org/10.1088/0022-3735/14/11/012

[15] Bruck, H. A., McNeill, S. R., Sutton, M. A., Peters, W. H. (1989). Digital image correlation using Newton-Raphson method of partial differential correction. *Experimental Mechanics*, 29, 261-267. https://doi.org/10.1007/BF02321405

[16] Pan, B., Li, K., Tong, W. (2013). Fast, robust and accurate digital image correlation calculation without redundant computations. *Experimental Mechanics*, 53, 1277-1289. https://doi.org/10.1007/s11340-013-9717-6

[17] Ji, J., Zhang, X., Xie, W. (2003). Calculation of isometric cubic spline interpolation problem using MATLAB. *Journal of Sichuan University of Technology*, S1, 37-40. (in Chinese)

[18] Jiang, Y., Gong, X., Liu, D., Cheng, Y., Fang, C., Shen, X. (2021). EnlightenGAN: Deep light enhancement without paired supervision. *IEEE Transactions on Image Processing*, 30, 2340-2349. https://doi.org/10.1109/TIP.2021.3051462

[19] Guo, C., Li, C., Guo, J., Loy, C. C., Hou, J., Kwong, S., Cong, R. (2020). Zero-reference deep curve estimation for low-light image enhancement. In *2020 IEEE/CVF Conference on Computer Vision and Pattern Recognition (CVPR)*. IEEE, 1780-1789. https://doi.org/10.1109/CVPR42600.2020.00185

[20] Ma, L., Ma, T., Liu, R., Fan, X., Luo, Z. (2022). Toward fast, flexible, and robust low-light image enhancement. In *2022 IEEE/CVF Conference on Computer Vision and Pattern Recognition (CVPR)*. IEEE, 5637-5646. https://doi.org/10.1109/CVPR52688.2022.00555

[21] Land, E. H., McCann, J. J. (1971). Lightness and retinex theory. *Journal of the Optical Society of America*, 61 (1), 1-11. https://doi.org/10.1364/JOSA.61.000001

[22] Wang, Y., Wan, R., Yang, W., Li, H., Chau, L.-P., Kot, A. (2022). Low-light image enhancement with normalizing flow. In *Proceedings of the AAAI Conference on Artificial Intelligence*, 36 (3), 2604-2612. https://doi.org/10.1609/aaai.v36i3.20162

[23] Pan, B., Yu, L., Wu, D. (2007). Research on speckle pattern production and evaluation techniques for digital image correlation methods. *Journal of Experimental Mechanics*, 22 (4), 448-454. (in Chinese)

[24] Liu, X., Qin, X., Li, R., Kong, Q., Gao, S., Li, Q., Guo, Q., Wu, X. (2021). Quality assessment of speckle subimage based on entropy in digital image correlation method. *Machine Tool & Hydraulics*, 49 (7), 48-51. (in Chinese) https://doi.org/10.3969/j.issn.1001-3881.2021.07.009

[25] Zhou, P., Goodson, K. E. (2001). Subpixel displacement and deformation gradient measurement using digital image/speckle correlation. *Optical Engineering*, 40 (8), 1613-1620. https://doi.org/10.1117/1.1387992

Received January 25, 2026
Accepted August 25, 2026